Accepted Manuscript

Geophysical methods applied to Quaternary studies in glacial environments: Rio valdez outcrop, Tierra del Fuego, Argentina

Claudia B. Prezzi, María J. Orgeira, Andrea M.J. Coronato, Diego R.A. Quiroga, Juan F. Ponce, Pablo A. Núñez Demarco, Pedro Palermo

PII: S1040-6182(18)30900-5

DOI: https://doi.org/10.1016/j.quaint.2019.07.022

Reference: JQI 7950

To appear in: *Quaternary International*

Received Date: 17 July 2018

Revised Date: 15 July 2019

Accepted Date: 15 July 2019

Please cite this article as: Prezzi, C.B., Orgeira, Marí.J., Coronato, A.M.J., Quiroga, D.R.A., Ponce, J.F., Núñez Demarco, P.A., Palermo, P., Geophysical methods applied to Quaternary studies in glacial environments: Rio valdez outcrop, Tierra del Fuego, Argentina, *Quaternary International* (2019), doi: https://doi.org/10.1016/j.quaint.2019.07.022.

GEOPHYSICAL METHODS APPLIED TO QUATERNARY STUDIES IN GLACIAL ENVIRONMENTS: RIO VALDEZ OUTCROP, TIERRA DEL FUEGO, ARGENTINA

Claudia B. Prezzi[1], María J. Orgeira[1], Andrea M. J. Coronato[2], Diego R. A. Quiroga[3], Juan F. Ponce[3], Pablo A. Núñez Demarco[4], Pedro Palermo[5]

1 CONICET – Universidad de Buenos Aires. IGeBA, Dpto. de Cs. Geológicas, Fac. de Cs. Exactas y Naturales. Ciudad Universitaria, Pabellón 2, CABA, C1428EGA, Argentina.
prezzi@gl.fcen.uba.ar
2 CONICET -CADIC. B. Houssay 200, (9410) Ushuaia, Tierra del Fuego, Argentina.
ICPA-UNTDF. Walanika 250, (9410) Ushuaia, Tierra del Fuego, Argentina.
3 CONICET -CADIC. B. Houssay 200, (9410) Ushuaia, Tierra del Fuego, Argentina.
4 CONICET. IGeBA, Dpto. de Cs. Geológicas, Fac. de Cs. Exactas y Naturales. Ciudad Universitaria, Pabellón 2, CABA, C1428EGA, Argentina.
5 CONICET. CIFICIEN. Facultad de Cs. Exactas, Universidad del Centro de la Provincia de Bs. As. Pinto 399, Tandil, Prov. de Bs. As., CP B7000GHG, Argentina.

ABSTRACT

In the Río Valdez mouth, located in the southeastern coast of Fagnano lake, Tierra del Fuego, an outcrop of 7 m thick lacustrine sediments was identified. Taking into account geomorphological and sedimentological surveys, such outcrop was interpreted as a rhythmic glacio-lacustrine deposit, formed in a frontal morainic complex during the Pleistocene. Ground magnetic and resistivity surveys were carried out, trying to determine the thickness and areal extension of these lacustrine sediments. A maximum E-W extension of ~ 220 m and a minimum NNW-SSE one of ~ 180 m were determined. A minimum thickness of ~ 20 m was estimated. Taking into account this thickness and an assumed average sedimentation rate, the natural dam that promoted the paleolake and their related lacustrine sediments could have existed previously to MIS 2, when the Last Glacial Maximum took place in the region. The applied geophysical methods proved to be a powerful tool for the investigation of palaeo-lake deposits.

Keywords: magnetic and resistivity surveys, palaeo-lake, rhythmites, MIS4, southernmost South America

INTRODUCTION

Fagnano lake valley, located in the Isla Grande de Tierra del Fuego center, is one of the most important glacial landform areas in southernmost South America. Extensive glaciated surfaces and a large ice volume contained by a glaciers network originating from the Cordillera Darwin covered the region during the Last Glacial Maximum (LGM), ca. 25 ka (Coronato et al. 2009, Waldman et al. 2010, Esteban et al. 2014). This large paleoglaciers landscape preserves paleoclimatic information from the southern extreme of

the continent, being extremely important to gain deeper insight into its paleogeographic and paleoenvironmental evolution. The mapping and analysis of glacial deposits and landforms constitute an important tool to understand and reconstruct glacial events (e.g. Coronato et al. 2002, 2009). In this connection, geophysical surveys can help to determine the thicknesses and areal extension of deposits originated by paleoglacier systems, contributing to a better knowledge of its development. Fagnano lake area has been investigated by different authors (e.g. Lippai et al. 2004, Lodolo et al. 2007, Peroni et al. 2007, 2008, 2011, Waldmann et al. 2008, Esteban et al. 2011, 2014, González Guillot et al. 2012), who used distinct geophysical methods.

Particularly, close to the mouth of Río Valdez, at the southern coast of Fagnano lake (54° 35' S; 67°20' W) beside a main road (Fig. 1), a 7-8 m thick deposit of lacustrine sediments crops out. It develops at 62 m a.s.l. and 25 m above the lake shore. It forms a plain placed in between a morainic complex. Based on geomorphological and sedimentological characteristics, the studied outcrop is interpreted as a glacio-lacustrine plain formed by rhythmites deposited among moraines. This ice-marginal paleo-lake would have been originated in a contact zone among paleo-Fagnano and tributary paleoglaciers flowing from the Lucio López Ranges (Coronato et al. 2009). The presence of dropstones suggests that this deposit is an ice-contact lake.

The objective of this paper is to reveal the volume and thickness of the sedimentary deposits that conform the glacio-lacustrine plain located close to Río Valdez mouth, which were described in an alongside road outcrop. The reconstruction of the size and shape of this paleo-lake can help to the interpretation of glacial paleogeography in central Tierra del Fuego. To accomplish this objective, ground magnetic and resistivity surveys were carried out. It is important to mention that previously published geophysical

studies (e.g. Lippai et al. 2004, Lodolo et al. 2007, Peroni et al. 2007, 2008, 2011, Waldmann et al. 2008, Esteban et al. 2011, 2014, González Guillot et al. 2012) do not include Río Valdez area and/or do not have enough resolution.

GEOLOGIC SETTING

Although there are not bare rock outcrops in the studied area, the presence of metasedimentary rocks of Beauvoir Formation is inferred. They would surround the widely spread Quaternary glacial deposits (Olivero et al. 2007). The Beauvoir Formation is composed by marine meta-sedimentary rocks as black slates, marls and tuffs (Capaccioni et al. 2013) of Early Cretaceous age. Most of the beds are massive, but there are some rhythmites composed by very fine to fine sandstones and mudstones (Olivero and Martinioni 2001). The above mentioned meta-pelites of Beauvoir Fm were intruded by back-arc plutonic rocks, representative of the Fuegian Potassium Magmatism. These plutonic rocks outcrop few kilometers to the northeast, at Cerro Jeujepen (González Guillot and Acevedo, 2009). They correspond to an igneous body mainly composed by hornblendites, pyroxenites, gabbros, diorites and monzonites (González Guillot and Acevedo 2009, González Guillot et al. 2012). According to Tassone et al. (2005), the large igneous body would reach depths of up to 8 km.

During the late Pleistocene a glacier originating from the Cordillera Darwin expanded eastwards through the Magallanes-Fagnano depression, now occupied by the Fagnano lake (26 m a.s.l.). The outlet glacier, flowing eastwards from the Darwin Cordillera, was fed by more than fifty tributary glaciers. An alpine-type landscape, including erosional landforms, developed in the western part of the present Fagnano lake. On the other hand, a piedmont-type landscape, including lateral moraines, glacio-fluvial

and glacio-lacustrine terraces, developed in the eastern region. The external front of this paleoglacier reached a maximum advance of 35-40 km to the northeast of its present-day easternmost head (Caldenius 1932). Such maximum advance is only poorly recognizable by the remnants of eroded moraines (Coronato et al. 2009). On the contrary, lateral and basal moraines, kames, knobs and kettles and glaciofluvial plains are quite well distributed and preserved, allowing the interpretation of glacier recessional phases (Coronato et al. 2002, 2009). This glacial landscape represents the Last Glacial Maximum (LGM) event and its first recessional phase, ca. 25 ka and 18 ka BP, respectively, during the Marine Isotope Stage (MIS) 2 (Coronato et al. 2002, 2009, Rabassa et al. 2011, Rutter et al. 2012). To the south, Cerro Jeujepen blocked the flow of tributary glaciers flowing from the Lucio López Range and forced the junction with the Fagnano paleo-glacier at Río Valdez area. There, basal moraines extend up to 2.5 km from the lake shore with elevations of 120 m a.s.l. and continue beside the lake coast, up to its eastern head. They are composed by till underlaid by glacio-deltaic deposits of Middle Pleistocene age (Bujalesky et al. 1997). Fossil peat contained in the lower units of till yielded 14C dates of 31,000 ± 510 – 48,200 ± 3300 years BP (Coronato et al. 2009), indicating that the ice covered this region before the LGM. These dating assays were made at the NSF Arizona AMS Facility, Arizona University (Coronato et al. 2009). A terminal morainic complex formed by arched hills was identified close to the Fagnano lake coast, surrounding the Río Valdez mouth and the therein glacio-lacustrine studied deposit. Since the bathymetry of this part of the lake shows shallow depths, it was interpreted that the moraine ridges continue under the lake, pointing to the occurrence of a frontal position during a recessional stage (Waldmann et al. 2010). Basal moraines separate the lake shore from the interior kames, glacio-fluvial and glacio-lacustrine plains, which were originated by the smaller, recessional, tributary glaciers.

Based upon the dip and strike of the sandy beds at the base of Cerro Jeujepen, Coronato et al. (2002) interpreted them as meltwater stream deposits coming from the tributary paleoglaciers during its recession. Radiocarbon dates from basal peats located in the surroundings show that most of the region was free of ice by 12,300 years BP. This zone was one of the most extensive glacially covered areas of Tierra del Fuego Island, at the southernmost of South America (Rabassa et al. 2011).

The studied outcrop is composed by 7 m of laminated silty-clay sediments with low content of laminated sands, overlaid in erosive boundary by 4.25 m of chaotic gravels in a silty matrix (Fig. 2a) corresponding to till. Each pair of rhythmites show sets of 2 cm thick dark clay and 0.5 cm thick light silts (Fig. 2b). Convolute laminations are only present at 2.75-3 m from the base.

METHODOLOGY

As mentioned above, geophysical studies including regional magnetic maps have been previously published (e.g. Peroni et al. 2007, 2008, 2011, González Guillot et al. 2012), but they do not include Río Valdez area and/or do not have enough resolution.

Magnetic anomalies arise from both an induced magnetization component and a remanent magnetization component. This is due to the Earth's magnetic field interacting with the magnetic susceptibility of the geologic body, and to the intensity and direction of the palaeomagnetic remanence of such body, respectively.

The total magnetic field was observed at 1380 magnetic stations, with a Geometrics 856 proton magnetometer. The spacing between stations along profiles was approximately 3 m. Three or more observations were taken at each station, and the corresponding values were averaged. Accurate position of each station was determined by

GPS. At regular time intervals (every hour), a base station located in the surveyed area was revisited in order to obtain control on the diurnal variation in the Earth's magnetic field. Then the corresponding IGRF (International Geomagnetic Reference Field) value was subtracted.

A grid of the calculated anomaly was produced applying "minimum curvature", a geostatistical gridding method. A grid cell size of approximately 3 m x 3 m was used. 3D Euler deconvolution was applied to magnetic anomalies in order to provide preliminary information of the depth distribution of the punctual sources. This method is based on Euler's homogeneity equation (Reid et al. 1990, Reid et al. 2003, Salem and Smith 2005). In order to solve Euler's equation, horizontal and vertical gradients of potential field data are required, which were calculated in the frequency domain (Gunn 1975). For the study area, we calculated Euler source points with SI = 1 and window sizes of 35 and 70 m using the software Oasis Montaj (Geosoft Inc.). The SI value was chosen, among the possible ones, considering that it corresponds to the 3D geometric shape that can better represent the studied glacio-lacustrine deposit. The window sizes used correspond to about half the anomalies width. Magnetic data were also analyzed to determine the depth to the top of the magnetic source layer by power density spectra methods developed by Spector and Grant (1970) and improved by Blakely (1996), Okubo et al. (1985) and Tanaka et al. (1999). Since we are attempting to determine only the top of the magnetic layer, there are no differences if the magnetic source is homogeneous or layered (Ravat et al. 2007). We applied a semi-automatic self-developed program to perform the analysis (Núñez Demarco et al. 2017).

Tilt derivatives of the upward continued reduced to the pole magnetic anomalies were also calculated with the aim of facilitating the location of contacts between different

171 geological units. Pole reduction transforms the magnetic field to a fictitious magnetic pole,
172 centering the magnetic anomalies on the causing bodies. Upward continuation of the
173 reduced to the pole magnetic anomalies up to 10 m was carried out in order to reduce the
174 very short-wavelength data noise, which would be amplified by the derivatives calculation.
175 3D susceptibility models were developed in order to explore the nature of the
176 bodies responsible for the detected magnetic anomalies. The magnetic susceptibility of Río
177 Valdez lacustrine sediments was determined by De Bernardi et al. (2013), it varies between
178 10 and 28 × 10^{-5} SI, showing an average value of ~14.1 × 10^{-5} SI. We collected 368
179 paleomagnetic oriented samples from Río Valdez glacio-lacustrine outcrop. Natural
180 remanent magnetization (NRM) intensities, declinations and inclinations were measured
181 with a Minispin (Molspin Ltd.) rotative magnetometer. Average intensity, declination and
182 inclination of NRM were calculated, obtaining values of 5.97 mA/m, 11° and -56.5°,
183 respectively, which were used in our 3D model. The corresponding Köenisberger ratio was
184 calculated (Table 1). Regarding the till layer, several authors published different values of
185 magnetic susceptibility for till deposits (e.g. 703 × 10^{-5} to 2388 × 10^{-5} SI (Parker Gay Jr.
186 2004); 24 × 10^{-5} to 113 × 10^{-5} SI (Vonder Haar and Hilton Johnson 1973), etc.).
187 Particularly, Parker Gay Jr. (2004) presented and discussed examples that cover a wide
188 range of possible magnetic anomaly types generated by different shapes and strikes of
189 magnetic glacial till sheets, highlighting the fact that till frequently has high magnetic
190 susceptibility values. An average magnetic susceptibility of 400 × 10^{-5} SI were used to
191 model the till layer covering the rhythmites. In order to attain a good fit between measured
192 and modeled anomalies, rock bodies to the east, west and beneath the glacial deposits were
193 introduced in the model, with magnetizations dominated by reverse NRMs (Table 1). These
194 bodies would correspond to the lower Cretaceous Beauvoir Formation (Martinioni et al.

2013), which outcrops to the east of the studied area in Cerro Jeujepen. As it was previously mentioned, these outcrops of Beauvoir Formation were intruded by the Jeujepen monzonite, which was paleomagnetically studied by Peroni et al. (2011) and Peroni (2012). These authors carried out magnetic susceptibility measurements for the Jeujepen monzonite, obtaining values ranging between 0.01 and 0.09 SI. In the case of Beauvoir Formation, magnetic susceptibility values ranged between 9.1×10^{-5} and 45×10^{-5} SI, with an average value of 30×10^{-5} SI (Peroni et al. 2011, Peroni 2012), which was the value used in our model. Unfortunately, there are not paleomagnetic data available for Beauvoir Formation. Therefore, we used a reverse NRM direction for Beauvoir Formation (Table 1), coincident with the lower Cretaceous reference direction for the studied area calculated from the Ponta Grossa Dike Swarm paleomagnetic pole (Solano et al. 2015). The modeling software IGMAS was used (Götze 1978, Götze and Lahmeyer 1988). IGMAS essentially uses triangulated polyhedrons to approximate areas of constant density and/or susceptibility within the Earth's crust and mantle. The numerical algorithms were developed by Götze (1984) and permit the calculation of gravity field and its gradients as well as magnetic field components and components of remnant and induced magnetic fields in one program step. The software package IGMAS eases the 3D interpretation of gravity and magnetic data bases. It uses an interoperable 3D Geoinformation System (IOGIS) and its functions (e.g. data queries, interoperability, visualization and interdisciplinary interpretations in an object-oriented data environment) to integrate other geophysical models, information, and data from both geophysics and geology (Schmidt and Götze 1999, Breunig et al. 2000). The initial geometries of the 3D modeled bodies are predefined by the user on a series of parallel vertical cross-sections. The automated triangulation of model surfaces between the parallel vertical cross-sections, allows the construction of complicated model geometries.

The optimal fit between observed and calculated anomalies is achieved during forward modeling by iterative geometry changes introduced by the user, according to the constraining information incorporated in the IOGIS. Following, the user manually modifies the geometry of the different bodies composing the 3D model, in view of the additional geological and geophysical information integrated in the model. The final model should minimize the differences between observed and calculated anomalies (i.e. residual anomalies). Residual anomalies should have lower amplitude than the estimated error in the observed anomaly and should show a tight concentration around zero with low standard deviation.

Resistivity surveys aim to determine the resistivity distribution in the subsurface by making measurements along the ground surface. It is based on measuring the voltage between a pair of electrodes caused by direct current injection between another pair of electrodes. There are many different electrode array configurations available, but all configurations are aimed at gathering data that can be used to estimate lateral and vertical variations in ground resistivity values. Resistivity surveys can be used to map geologic variations, including lithology (e.g., clay versus gravel), presence of ground water, fracture zones, etc. It was not possible to carry out electrical resistivity tomographies because the studied zone is covered by a very dense forest, which hindered the application of this technique. Instead, five vertical electrical soundings (VES) were carried out in the study area using a digital resistivity meter GEOMETER MPX-400 (Ponti Electronics) and a Schlumberger electrode array. The position of each one of the VES points was determined using GPS. The potential electrodes separation was of 3 m and the maximum current electrode separation was of 80 m. The five VES were projected along a NE-SW trending profile. An inverse 2D model of resistivity distribution along the profile was numerically

obtained in the form of a simple rectangular cell model using the software RES2DINV of Geotomo (Loke 1996-2002, Loke 2001). This program allows an estimation of the cells resistivity that adjusts the quantities measured at surface, within certain discrepancy. During the inversion routine the initial model parameters are modified and improved by solving a least-squares equation (Lines and Treitel 1984). The discrepancy between the calculated values of apparent resistivity and those inferred from field data are expressed through the root mean square (RMS). Finally, a contour diagram showing the resistivity distribution of the modeled profile is obtained.

RESULTS

A 3D forward magnetic model was developed in order to investigate the geometry of the glacio-lacustrine sediments.

The magnetic anomalies (Fig. 3) show maximum values (of approximately −88 to −120 nT) at the centre of the surveyed area (~ X: 607280-607440 m (UTM zone 19S)). Such maximum values define an elongated zone trending NNE-SSW. These maximum values are flanked by minimum ones to the E and W (~ X: 607440-607480 m and ~ X: 607220-607280 m, respectively, (UTM zone 19S)), reaching values of – 138 to -200 nT (Fig. 3).

In Figure 4 we present the magnetic anomalies together with the corresponding Euler solutions considering a SI of 1 and window sizes of 35 and 70 m. It can be observed that most of the solutions are located below the elongated magnetic maxima, at average depths ranging between approximately 3–7 m (Fig. 4). In connection, to the E and W of the magnetic maxima, Euler solutions are concentrated below the high gradient transition zones to the magnetic minima, at average depths ranging between approximately 11–20 m (Fig.

4). However, it should be noticed that Euler source points are mathematical fictions and do not point to real geological point masses. Consequently, it should be taken into account that Euler calculations could not actually portray real distributions of magnetic material. We also calculated the depth to the top of the magnetic layer for 35 x 35 m square windows with an overlap of 33.25 m (95%), using 2D power density spectra methods. We found that for the studied region, the depth to the top of the magnetic layer varied between 11 and 22 m (Fig. 5).

The tilt derivative and the horizontal derivative of the tilt derivative of the upward continued reduced to the pole magnetic anomalies, allowed to determine the location of the contacts of the glacial deposits (Fig. 6a and 6b). In the case of the tilt derivative, the contacts are located below the cero contour line (Fig. 6a) (Verduzco et al. 2004). On the other hand, the maximum values of the horizontal derivative of the tilt derivative would delineate the contacts (Fig. 6b) (Verduzco et al. 2004).

Figure 7 displays the location of the five vertical electrical soundings (VES) carried out in the study area. These five VES were integrated to produce a NE-SW 2D cross-section (Fig. 7). The corresponding measured and calculated apparent resistivity pseudosections and the resulting resistivity inverse model can be seen in Figure 8. From this model, the existence of a layer with very high resistivities, ranging between ~ 300 and 3000 ohm.m, can be identified to the top of the cross-section with a thickness of ~ 5-9 m. Below this layer, a very low resistivity zone, with resistivity values ranging between ~50 and 200 ohm.m and extending down to at least 20 m depth, is observed (Fig. 8).

In the 3D forward magnetic model an initial thickness of approximately 5 m and an average magnetic susceptibility of 4×10^{-3} SI were used to model the till layer covering the rhythmites (Table 1). Such initial thickness is in accordance with the thickness

291 measured in the outcrop. The glacio-lacustrine deposits underlying the till were modeled
292 using the susceptibility and measured NRM parameters shown in Table 1. With the aim of
293 reducing the ambiguity and the uncertainty inherent to the magnetic method, certain aspects
294 of the susceptibility structure during the forward modeling were fixed. Thereby, the
295 minimum thickness, magnetic susceptibility and NRM parameters assigned to the till and
296 rhythmites bodies were predetermined and were not changed. In order to attain a good fit
297 between measured and modeled anomalies, rock bodies to the east, west and beneath the
298 glacial deposits were introduced in the model, with magnetizations dominated by reverse
299 NRMs (Table 1). Our model is composed of 10 parallel E-W sections extending down to 50
300 m. Figure 9 shows five of such sections, displaying measured and calculated anomalies and
301 the corresponding subsurface susceptibility structure. The forward modeled 3D
302 susceptibility structure thoroughly reproduces the measured magnetic field. The residual
303 magnetic anomaly depicts the differences between measured and modeled anomalies (Fig.
304 10). Only less than ~5% of the study area presents residual anomalies greater than ± 5 nT
305 (Fig. 10). These anomalies are of very short wave length and not systematically distributed
306 across the map. Residual anomaly values are tightly concentrated around 0 nT, with a
307 standard deviation of 3.84 nT and a correlation coefficient of 0.97. These results suggest
308 that our model satisfactorily represents the magnetic susceptibility and NRM parameters
309 distribution in the studied area. A 3D view of the measured magnetic anomaly and the
310 modeled 3D structure is showed in Figure 11.
311
312 DISCUSSION

The applied geophysical methods are a powerful tool that allowed the estimation of the till and glacio-lacustrine sediments thicknesses and their areal extension in comparison with their surficial morphology.

The magnetic maxima would coincide with the presence of the glacio-lacustrine deposits. The high gradient transition zones to the magnetic minima to the E and W would indicate the contacts depicting the extension of such deposits. Most of Euler solutions are located below the elongated magnetic maxima, at average depths ranging between approximately 3–7 m (Fig. 4). These depths of Euler solutions would be in agreement with the average thickness of around 4 m documented for the till layer covering the glacio-lacustrine sediments in Río Valdez outcrop (Fig. 2a). Euler solutions are also concentrated below the high gradient transition zones at average depths ranging between approximately 11–20 m (Fig. 4). Spectral methods results agree notably well with the Euler solutions.

In order to attain a good fit between measured and modeled anomalies, rock bodies to the east, west and beneath the glacial deposits were introduced in the model, with magnetizations dominated by reverse NRMs (Table 1). These bodies would correspond to the lower Cretaceous Beauvoir Formation (Martinioni et al. 2013), which outcrops to the east of the studied area in Cerro Jeujepen. We used a value of magnetic susceptibility of 3 x 10^{-4} SI (Peroni et al. 2011, Peroni 2012) for Beauvoir Formation. Considering the magnetic susceptibility of the glacio-lacustrine deposits and the parameters used to model Beauvoir Formation (Table 1), the depth to the top of the magnetic layer obtained from spectral methods (Fig. 5) would coincide with the base of the glacio-lacustrine deposits and the top of Beauvoir Formation. From the 3D magnetic model, isopach maps of the till and rhythmites deposits and an isochoric map of the base of the rhythmites were obtained. The thicknesses were compared with the contacts determined from the tilt derivatives (Fig. 12a

and b). It can be observed that there is a good correlation between thicknesses less than 2-5 m and the 0 and maximum values of the tilt derivative and the horizontal derivative of the tilt derivative, respectively (Figs. 6b, 12a and b). Particularly, in the case of the horizontal derivative of the tilt derivative, maximum values in the center of the studied area coincide with the maximum till thickness, which rapidly decreases to the east and west (Figs. 6a and 12a). Furthermore, the till isopach map (Fig. 12a) and the isochoric map of the base of the rhythmites (Fig. 12c) agree notably well with Euler solutions depths (4-7 m for till, 9-20 m for rhythmites) and the depth to the base of the rhythmites calculated applying power density spectra methods (maximum depth of 21-22m) (Fig. 5). These facts suggest that our 3D magnetic model is a robust characterization of the subsurface distribution of the glacial sedimentary units.

The location of the glacial deposits contacts, determined from the tilt derivatives of the magnetic anomalies, 3D magnetic modelling and Euler deconvolution, indicates their extension. Such deposits would have a maximum E-W extension of ~ 220 m and a minimum NNW-SSE extension of 180 m. The maximum NNW-SSE extension could not be determined because to the south of the surveyed area there are buildings, fences, pipes, etc., that would introduce considerable noise in the magnetic measurements. The till sheet would have an average thickness of approximately 5-6 m, reaching maximum values of 10-11 m to the south of the studied area.

In the case of the resistivity inverse model, the high resistivity layer would correspond to the till deposit that covers the glacio-lacustrine sediments, which, in turn, would be depicted by the low resistivity zone. The till thickness deduced from the inverse resistivity modeling coincides with the depths obtained through Euler deconvolution and power density spectra methods of the magnetic anomalies. A minimum thickness of

361 approximately 11- 15 m is estimated for the glacio-lacustrine sediments, in agreement with
362 Euler deconvolution and power density spectra methods. It is important to highlight that it
363 was not possible to reach the necessary investigation depths to estimate the real thickness of
364 the rhythmites because the surveyed zone is covered by a dense forest, which hindered
365 attaining larger distances between current electrodes. However, Euler deconvolution,
366 spectral methods and 3D modelling of the magnetic anomalies provided coincident results,
367 suggesting an average thickness of the glacio-lacustrine deposits of approximately 20 m,
368 with maximum values of 22-23 m in the center of the studied area.

369 Unfortunately, there is no information about glacial sedimentation rates during the
370 Pleistocene in Tierra del Fuego that could help to constrain the age of this deposit.
371 Sedimentation rates of Potrok Aike lake (51°58' S- 70°22' O) can be used to make a rough
372 estimation of how long Río Valdez lake system was operative, assuming a continuous
373 sedimentation process of rhythmites and taking into account that Potrok Aike was not an
374 ice-marginal lake during Pleistocene. From the obtained thickness of 20 meters and
375 assuming an average sedimentation rate ranging between 0.37 and 8.5 mm/year, similar to
376 that of Potrok Aike lake (Kliem et al. 2013), it is possible to estimate the lapse involved
377 during the deposition of the studied glacio-lacustrine deposits. Considering that Río Valdez
378 sediments are rhythmites, we used the minimum sedimentation rate determined for Potrok
379 Aike lake of 0.37 mm/year, estimating that these deposits could represent a maximum
380 deposition lapse of 54,054 years. This estimation is in accordance with the fossil peat ages
381 obtained in the surrounding tills by Bujalesky et al. (1997) and Coronato et al. (2009).
382 Fossil peat contained in the lower basal till deposits in the area by Coronato et al. (2009)
383 yielded 14C dates of 31,000 ± 510 – 48,200 ± 3300 years BP. These dating assays were
384 made at the NSF Arizona AMS Facility, Arizona University (Coronato et al. 2009). This

data indicate that a glacial advance took place in the area prior to the Last Glacial Maximum (ca. 25,000–23,000 cal. years BP). Then, our hypothesis is consistent with previous findings in the area, which indicate that glaciers were present before MIS 2.

We propose that our results would suggest that the natural dam that promoted the paleolake and their related lacustrine sediments could have been active probably ca. 57,000 yrs BP, approximately near the boundary between MIS 3 and 4 (sensu Lisiecki and Raymo 2005). In order to further constrain the above mentioned hypothesis, absolute dates for Río Valdez deposits would be necessary.

CONCLUSIONS

A maximum E-W and a minimum NNW-SSE extension of Río Valdez glacial deposits of approximately 220 m and 180 m, respectively, were determined, increasing the surficial dimensions obtained by field and mapping surveys.

An average thickness of 20 m was estimated for the glacio-lacustrine deposits, while the overlying till sheet average thickness would be of 5-6 m.

From the geophysically obtained thickness, and assuming an average sedimentation rate of 0.37 mm/year (similar to that of Potrok Aike lake), we estimate that these deposits could represent a maximum deposition lapse of 54,054 years. This estimation is consistent with previous findings in the area, which indicate that glaciers were present before MIS 2.

We propose that our results would suggest that the natural dam that promoted the paleolake and their related lacustrine sediments could have been active probably ca. 57,000 yrs BP, approximately near the boundary between MIS 3 and 4.

These results reveal information not possible to obtain from the exposure outcrop and help to reconstruct palaeo-glaciological conditions in a glacial junction area. By the other side, they will help to calculate deposition rates once absolute dates are available.

This study demonstrates the usefulness of geophysical methods applied to Quaternary studies.

REFERENCES

Blakely, R. J., 1996. Potential theory in gravity and magnetic applications. Cambridge University Press.

Breunig, M., Cremers, A., Götze, H.-J., Seidemann, R., Schmidt, S., Shumilov, S., Siehl, A., 2000. Geologic mapping based on 3D models using an interoperable GIS. Geo-Information-Systems Journal of Spatial Information and Decision Making 13, 12–18.

Bujalesky, G.; Heusser, C.; Coronato, A.; Roig, C., Rabassa, J. 1997. Pleistocene glaciolacustrine sedimentation at Lago Fagnano, Andes of Tierra del Fuego, Southernmost South America. Quaternary Science Reviews, 16 (1-2):767-778.

Caldenius, C. 1932. Las glaciaciones Cuaternarias en Patagonia y Tierra del Fuego. Geografiska Annaler 14: 1-164.

Capaccioni, B., Menichetti, M., Renzulli, A., Tassone, A., Huertas, A., 2013. Thermal waters of 'tectonic origin': the alkaline, Na-HCO_3 waters of the Rio Valdez geothermal area (Isla Grande de Tierra del Fuego, Argentina). Geofluids 13, 21-31.

Coronato, A.; Roig, C.; Mir, X. 2002. Geoformas glaciarias de la región oriental del Lago Fagnano, Tierra del Fuego, Argentina. In: Cabaleri, N.; Cingolani, C.; Linares, E.;

López de Luchi, M. Ostera, H.; Panarello, H. (Eds.) Actas del XV Congreso Geológico Argentino, Tomo II, pp:457-462. CD-Rom. Artícle Nº 24, 6 pp.

Coronato, A., Seppälä, M., Ponce, J.F., Rabassa, J. 2009, Glacial geomorphology of the Pleistocene Lake Fagnano ice lobe, Tierra del Fuego, southern South America, Geomorphology, 112, 67-81.

De Bernardi, M., Gogorza, C., Orgeira, M., Coronato, A., Quiroga, D., 2013. Rock magnetic studies from the Rio Valdez paleolake outcrop (Tierra del Fuego, Argentina): preliminary results. Latinmag Letters, Volume 3, Special Issue (2013), PD05, 1-6. Proceedings Montevideo, Uruguay.

Esteban, F.D., Tassone, A., Menichetti, M., Rapalini, A.E., Remesal, M.B., Cerredo, M.E., Lippai, H., Vilas, J.F., 2011. Magnetic fabric and microstructures across the Andes of Tierra del Fuego, Argentina. Andean Geology 38 (1), 64-81.

Esteban, F., Tassone, A., Lodolo, E., Menichetti, M., Lippai, H., Waldmann, N., Darbo, A., Baradello, L., Vilas, F., 2014. Basement geometry and sediment thickness of lago Fagnano (Tierra del Fuego). Andean Geology 41 (2), 293-312.

González Guillot, M., Acevedo, R., 2009. Facies con biotita y granate en plutones de los Andes Fueguinos de Argentina. In: XII Congreso Geológico Chileno, Actas in CD. Santiago de Chile.

González Guillot, M., Prezzi, C., Escayola, M., Acevedo, R., 2012. A comparative study of two rear-arc plutons and implications for the Fueguian Andes tectonic evolution: Mount Kranck pluton and Jeu-Jepén monzonite, Argentina. Journal of South American Earth Sciences 38, 71-88.

453 Götze, H.-J., 1978. Ein numerisches Verfahren zur Berechnung der gravimetrischen Feldgr
454 aen drei- dimensionaler Modellkörper. Arch. Met. Geoph. Biokl., Ser. A, 25, 195-
455 215.
456 Götze, H.-J., 1984. Über den Einsatz interaktiver Computergraphik im Rahmen 3-
457 dimensionaler Interpretationstechniken in Gravimetrie und Magnetik.
458 Habilitationsschrift. Technische Universität Clausthal, Clausthal.
459 Götze, H.-J., Lahmeyer, B., 1988. Application of three-dimensional interactive modeling in
460 gravity and magnetics, Geophysics 53(8), 1096 - 1108.
461 Gunn, P., 1975. Linear transformations of gravity and magnetic fields. Geophysical
462 Prospecting, 23(2), 300–312.
463 Kliem, P., Enters, D., Hahn, A., Ohlendorf, C., Lisé-Pronovost, A., St-Onge, G.,
464 Wastegård, S., Zolitschka, B., PASADO science team, 2013. Lithology, radiocarbon
465 chronology and sedimentological interpretation of the lacustrine record from Laguna
466 Potrok Aike, southern Patagonia. Quaternary Science Reviews, 71, 54-69.
467 Lines, L.R., Treitel, S., 1984. A view of least-squares inversion and its application to
468 geophysical problems. Geophysical Prospecting 32, 159–186.
469 Lippai, H., Lodolo, E., Tassone, A., Hormaechea, J.L., Menichetti, M., Vilas, J.F., TESAC
470 Party, 2004. Morpho-structure of Lago Fagnano (Tierra del Fuego) and adjacent
471 areas. Bollettino di Geofísica Teorica ed Applicata 45 (2), 142-144.
472 Lisiecki, L. E., Raymo, M. E., 2005. A Pliocene-Pleistocene stack of 57 globally
473 distributed benthic δ18O records. Paleoceanography, 20(1),
474 doi:10.1029/2004PA001071.

475 Lodolo, E., Lippai, H., Tassone, A., Zanolla, C., Menichetti, M., Hormaechea, J.L., 2007.
476 Gravity map of the Isla Grande de Tierra del Fuego, and morphology of Lago
477 Fagnano. Geologica Acta 4, 307-314.
478 Loke, M.H., 1996–2002. Tutorial: 2-D and 3-D electrical imaging surveys. Geotomo
479 Software.
480 Loke, M.H., 2001. Rapid 2-D resistivity and IP inversion using the least-squares method.
481 Geoelectrical Imaging 2-D and 3-D. Geotomo Software.
482 Martinioni, D., Olivero, E., Medina, F., Palamarczuk S., 2013. Cretaceous stratigraphy of
483 Sierra the Beauvoir, Fueguian Andes, Argentina. Revista de la Asociación Geológica
484 Argentina, 70(1), 70-95.
485 Nüñez Demarco, P. A., Prezzi, C., Sánchez Bettucci, L., 2017. Un nuevo programa basado
486 en Matlab para análisis espectral de datos magnetométricos. Latinmag Letters Special
487 Issue, 7, GEP04, 1-6.
488 Okubo,Y., Graft, R. J., Hansent, R. O., Ogawa K., Tsu, H., 1985. Curie point depth of the
489 island of Kyushu and surrounding areas, Japan. Geophysics, 53(3), 481-494.
490 Olivero, E., Martinioni, D., 2001. A review of the geology of the Argentinian Fuegian
491 Andes. Journal of South American Earth Sciences, 14, 175-188.
492 Olivero, E. B., Malumián, N., Martinioni, D. R., 2007. Mapa Geológico de la Isla Grande
493 de Tierra del Fuego e Isla de los Estados; Provincia de Tierra del Fuego, Antártida e
494 Islas del Atlántico Sur; República Argentina (escala 1:500.000), SEGEMAR, Buenos
495 Aires.
496 Parker Gay Jr., S., 2004. Glacial Till: A Troublesome source of near-surface magnetic
497 anomalies. Applied Geophysics, Inc. Copyright © by S. Parker Gay, Jr. 2004. 71 pp.

Peroni, J., 2012. Modelado geofísico-geológico de plutones en las Islas Grande de Tierra del Fuego (Argentina) y Navarino (Chile). PhD Thesis, Facultad de Ciencias Exactas y Naturales, Universidad de Buenos Aires, Argentina. http://digital.bl.fcen.uba.ar/Download/Tesis/Tesis_5214_Peroni.pdf.

Peroni, J., Tassone, A., Lippai, H., Menichetti, M., Lodolo, E., Vilas, J. F., 2007. Geophysical modeling of the Kranck pluton. Tierra del Fuego. Argentina. In International Geological Congress on the Southern Hemisphere (Geosur 2), Abstracts book: p. 122. Santiago.

Peroni, J., Tassone, A., Menichetti, M., Lippai, H., Lodolo, E., Vilas, J. F., 2008. Geologia e geofisica del plutone Kranck (Lago Fagnano, Tierra del Fuego, Argentina). Rendiconti Online della Società Geologica Italiana 1, 132-136.

Peroni, J., Tassone, A., Cerrado, M. E., Bran, D., Lippai, H., Vilas, F. J., 2011. Prospección magnetométrica del plutón Jeujepen, Isla Grande de Tierra del Fuego, Argentina. In Latinmag Letters, Volume 1, Special Issue (2011), A03, 1-7. Proceedings Tandil, Argentina.

Rabassa, J., Coronato, A., Martínez, O., 2011. Late Cenozoic glaciations in Patagonia and Tierra del Fuego: an updated review. Biological Journal of the Linnean Sociecty, 103, 316-335.

Ravat, D., Pignatelli, A., Nicolosi, I., Chiappini, M., 2007. A study of spectral methods of estimating the depth to the bottom of magnetic sources from near-surface magnetic anomaly data. Geophysical Journal International, 169(2), 421-434.

Reid, A. B., Allsop, J., Granser, H., Millett, A., Somerton, I., 1990. Magnetic interpretation in three dimensions using Euler Deconvolution. Geophysics 55(1), 80-91.

521 Reid, A.B., FitzGerald, D., McInerney, P., 2003. Euler deconvolution of gravity data.
522 Society of Exploration Geophysicists (SEG), Annual Meeting, 2003, pp. 580-583.
523 Rutter, N., Coronato, A., Helmens, K., Rabassa, J., Zárate, M., 2012. Glaciations in North
524 and South America from the Miocene to the Last Glacial maximum: comparisons,
525 linkages and uncertainties. Springer Science & Business Media.67p.
526 Salem, A., Smith, R., 2005. Depth and structural index from normalized local wavenumber
527 of 2D magnetic anomalies. Geophysical Prospecting 53(1), 83-89.
528 Schmidt, S., Götze, H.-J., 1999. Integration of data constraints and potential field
529 modelling—an example from southern Lower Saxony, Germany. Physics and
530 Chemistry of the Earth (A) 24, 191–196.
531 Solano, M., Goguitchaichvili, A., Mena, M., Alva-Valdivia, L., Morales Contreras, J.,
532 Cejudo Ruiz, R., López Loera, H., Soler, A., Urrutia-Fucugauchi, J., 2015.
533 Paleomagnetic Pole Positions and Geomagnetic Secular Variation from the
534 Cretaceous Ponta Grossa Dike Swarm (Brazil). Geofísica Internacional 54(2), 167-
535 178.
536 Spector, A., Grant, F.S., 1970. Statistical Models for interpreting aeromagnetic data.
537 Geophysics, 35, 293-302.
538 Tanaka, A., Okubo, Y., Matsubayashi, O., 1999. Curie point depth based on spectrum
539 analysis of the magnetic anomaly data in East and Southeast Asia. Tectonophysics,
540 306(3), 461-470.
541 Tassone, A., Lippai, H., Lodolo, E., Menichetti, M., Comba, A., Hormaechea, J., Vilas, J.,
542 2005. A geological and geophysical crustal section across the Magallanes-Fagnano
543 fault in Tierra del Fuego. Journal of South American Earth Sciences 19, 99-109.
544 Verduzco, B., Fairhead, J.D., Green, C.M., MacKenzie, C., 2004. New insights

to magnetic derivatives for structural mapping. The Leading Edge 23, 116-119.

Vonder Haar, S., Hilton Johnson, W., 1973. Mean Magnetic Susceptibility: A useful parameter for stratigraphic studies of glacial till. Journal of Sedimentary Petrology 43(4), 1148-1151.

Waldmann, N., Ariztegui, D., Anselmetti, F.S., Austin, J.A. Jr., Dunbar, R.B., Moy, C.M., Recasens, C., 2008. Seismic stratigraphy of Lago Fagnano sediments (Tierra del Fuego, Argentina) - a potential archive of Paleoclimatic change and tectonic activity since the Late Glacial. Geologica Acta 6, 101-110.

Waldmann, N., Aristegui, D., Anselmetti, F., Coronato, A., Austin-Jr., J., 2010. Geophysical evidence of multiple glacier advances in Lago Fagnano (54°S), Southernmost Patagonia. Quaternary Science Reviews, 29 (9-10), 1188-1200.

ACKNOWLEDGMENTS

This research has been supported by PICT FONCYT 2012-0628 to A. Coronato. We thank to the owners of “El Valdez” farm who kindly allowed the access to their property. The reviews of an anonymous reviewer and of Dr. Marco Menichetti, and manuscript handling by Editor- in- Chief Professor van Kolfschoten are also very appreciated.

FIGURE CAPTIONS

Figure 1: Satellite images showing the location of the studied zone. White dots: magnetic stations. A labelled black rectangle: geophysically surveyed area.

569 Figure 2: a) Outcrop of the studied glacial deposits at Río Valdez mouth. A brown
570 yellowish till sheet, with a thickness of 4-5 m, covers the 7 m thick gray rhythmites. b)
571 Lamination of the glacio-lacustrine rhythmic deposits.
572
573 Figure 3: Magnetic anomaly detected in the studied area. Black dots: magnetic stations.
574 Location of surveyed area is shown in Figure 1 (A labelled black rectangle).
575
576 Figure 4: a) Euler solutions laid over the magnetic anomaly, calculated using a SI=1 and a
577 window size of 35 m. b) Euler solutions laid over the magnetic anomaly, calculated using a
578 SI=1 and a window size of 70 m. Location of surveyed area is shown in Figure 1 (A
579 labelled black rectangle).
580
581 Figure 5: Depth to the top of the magnetic layer (i.e. depth to the base of the glacio-
582 lacustrine deposits outcropping in Río Valdez) obtained through power density spectra
583 methods, using 35x35m square windows with an overlap of 95%. Location of surveyed
584 area is shown in Figure 1 (A labelled black rectangle).
585
586 Figure 6: a) Tilt derivative of the upward continued reduced to the pole magnetic
587 anomalies, showing the location of the contacts of the glacial deposits through the 0
588 contour lines. Black lines: 0 contour lines. b) Horizontal derivative of the tilt derivative of
589 the upward continued reduced to the pole magnetic anomalies, showing the location of the
590 contacts of the glacial deposits through its maximum values. Black lines: maximum values
591 contour lines. Location of surveyed area is shown in Figure 1 (A labelled black rectangle).
592

593 Figure 7: Magnetic anomalies detected in the study area showing the location of the five
594 VES carried out. White numbers: location of each VES. Black arrow: cross-section along
595 which the VESs were integrated. Location of surveyed area is shown in Figure 1 (A
596 labelled black rectangle).
597
598 Figure 8: a) Top: measured apparent resistivity pseudosection. Middle: calculated apparent
599 resistivity pseudosection. Bottom: inverse resistivity model section. Black arrows: location
600 of each VES. b) Vertical exaggerated inverse resistivity model section.
601
602 Figure 9: Parallel E-W vertical sections composing our 3D forward magnetic model of the
603 study area. Continuous green line: measured magnetic anomaly, Dashed green line:
604 modeled magnetic anomaly.
605
606 Figure 10: Residual magnetic anomaly of the studied area. Black lines: contour lines.
607
608 Figure 11: 3D view of the magnetic model of the study zone, showing measured magnetic
609 anomaly.
610
611 Figure 12: a) Isopach map of the till deposits overlaid by the Euler solutions calculated
612 using a SI=1 and a window size of 70 m. Orange line: 0 contour line of the tilt derivative of
613 the upward continued reduced to the pole magnetic anomalies. b) Isopach map of the
614 glacio-lacustrine rhythmic deposits. Orange line: 0 contour line of the tilt derivative of the
615 upward continued reduced to the pole magnetic anomalies. c) Isochoric map of the base of
616 the glacio-lacustrine rhythmic deposits overlaid by the Euler solutions calculated using a

SI=1 and a window size of 70 m. Orange line: 0 contour line of the tilt derivative of the upward continued reduced to the pole magnetic anomalies. Location of surveyed area is shown in Figure 1 (A labelled black rectangle).

Table 1: Declination and inclination of the natural remnant magnetization, magnetic susceptibility and Köenisberger ratio of the different geologic units considered in the 3D forward magnetic model.

Bodies	Natural Remanent Magnetization		Susceptibility	Köenisberger
	Declination (°)	Inclination (°)	SI	Ratio
Till sheet	0	0	0.004	0
Glacio-lacustrine deposits	11	-56.5	0.000141	3.13
Beauvoir Formation east	183	71	0.0003	20
Beauvoir Formation west	183	71	0.0003	1
Beauvoir Formation beneath	183	71	0.0003	20

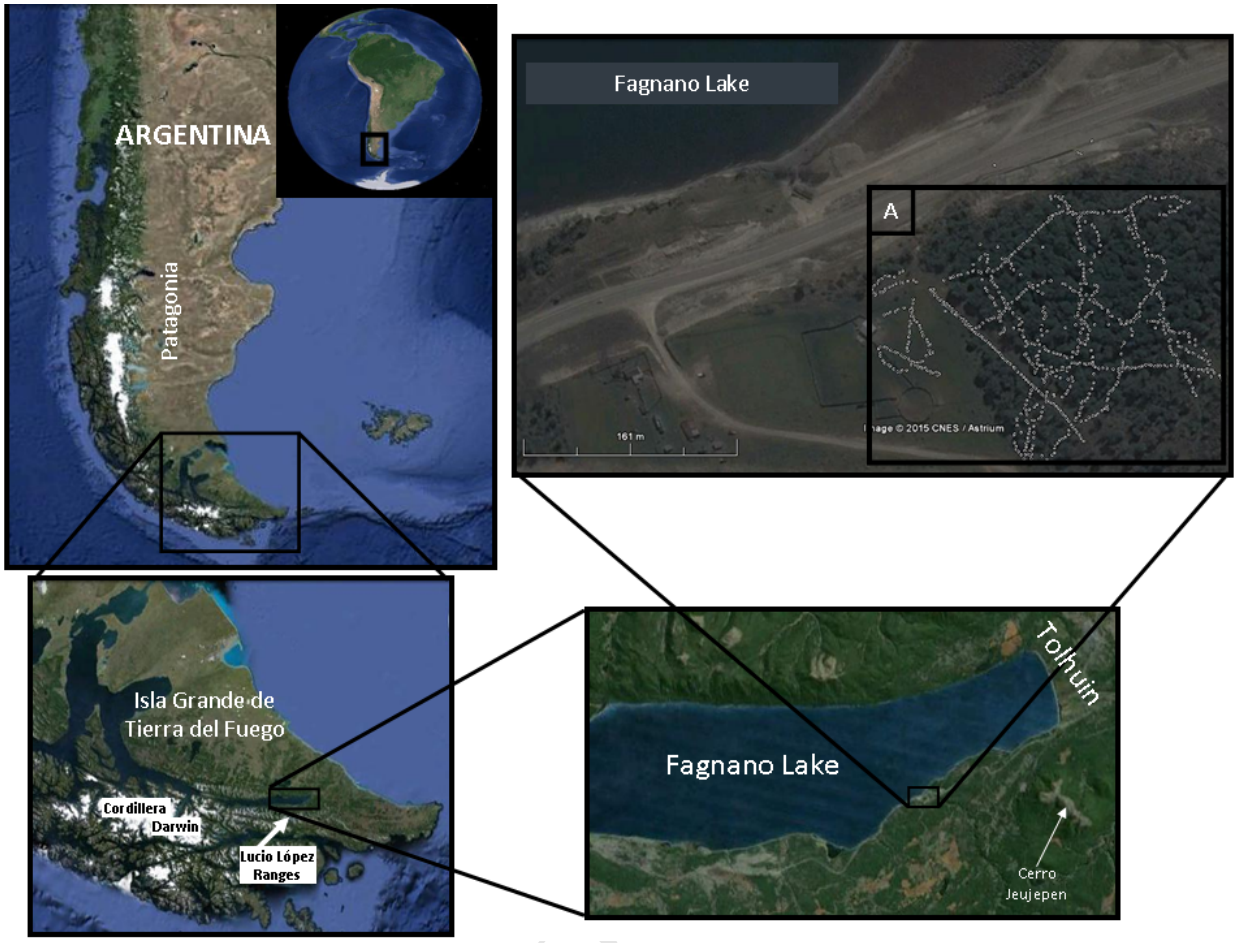
ARGENTINA
Patagonia
Fagnano Lake
A
161 m
Isla Grande de
Tierra del Fuego
Cordillera
Darwin
Lucio López
Ranges
Fagnano Lake
Tolhuin
Cerro
Jeujepen

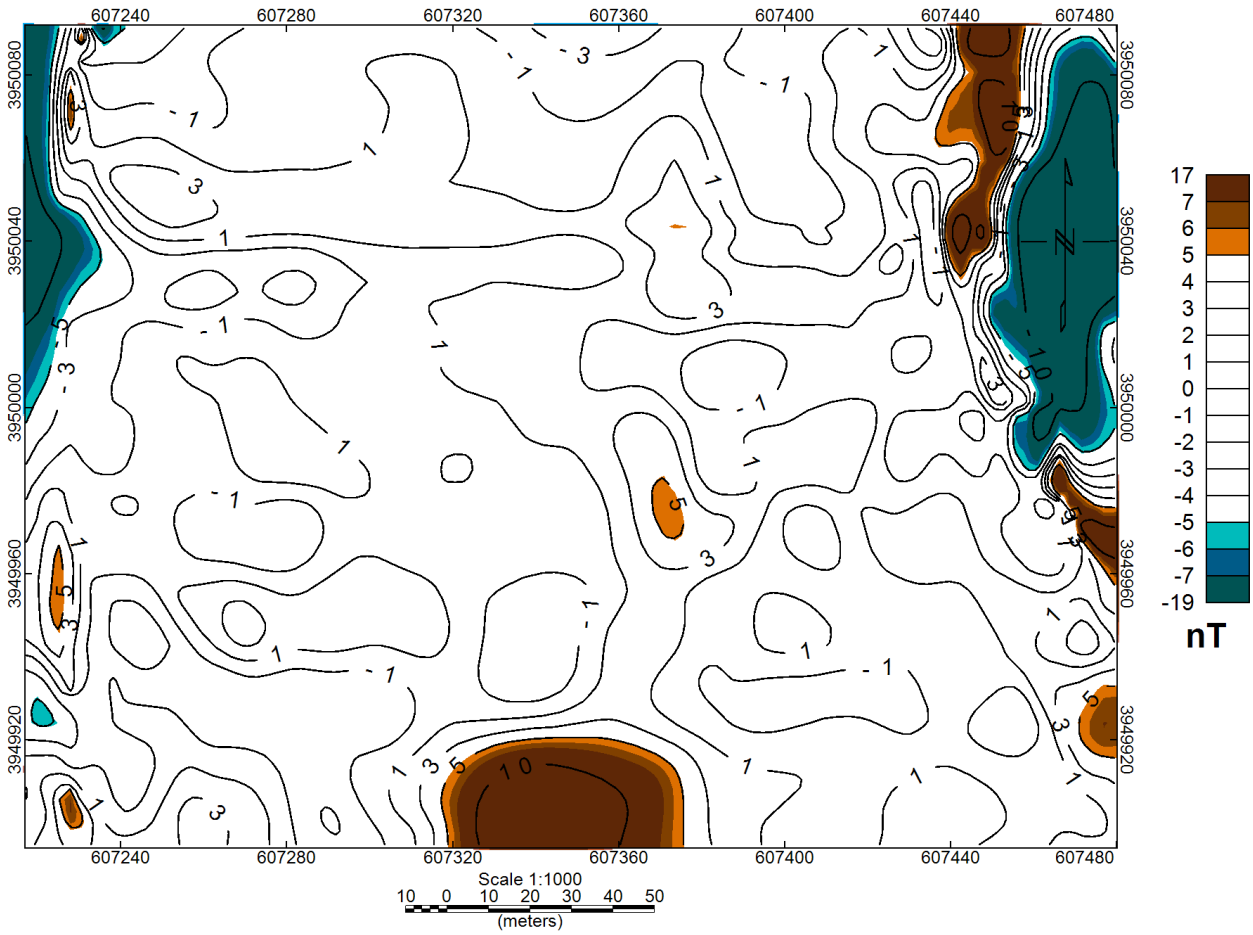
607240
607280
607320
607360
607400
607440
607480
3950080
3950040
3950000
3949960
3949920
N
17
7
6
5
4
3
2
1
0
-1
-2
-3
-4
-5
-6
-7
-19
nT
Scale 1:1000
10 0 10 20 30 40 50
(meters)

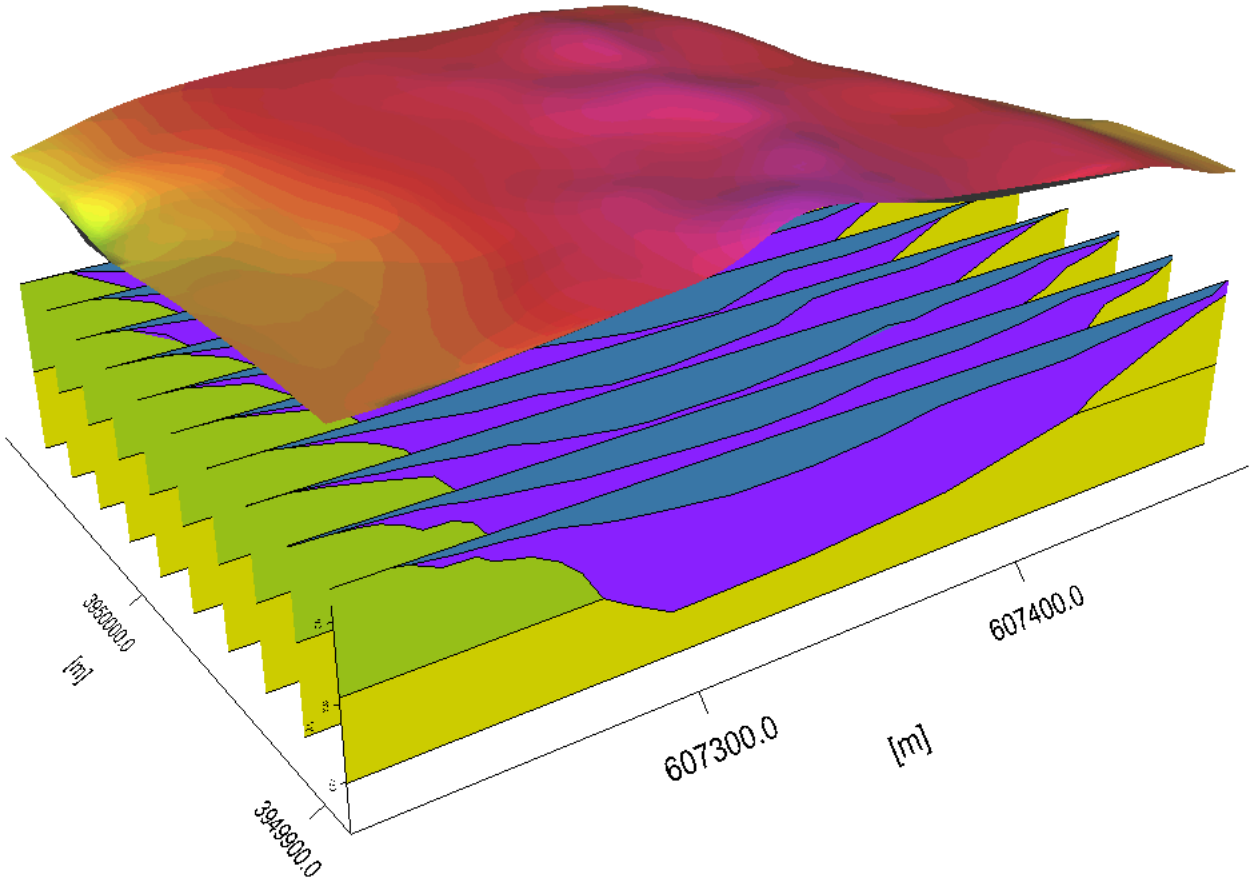

a)

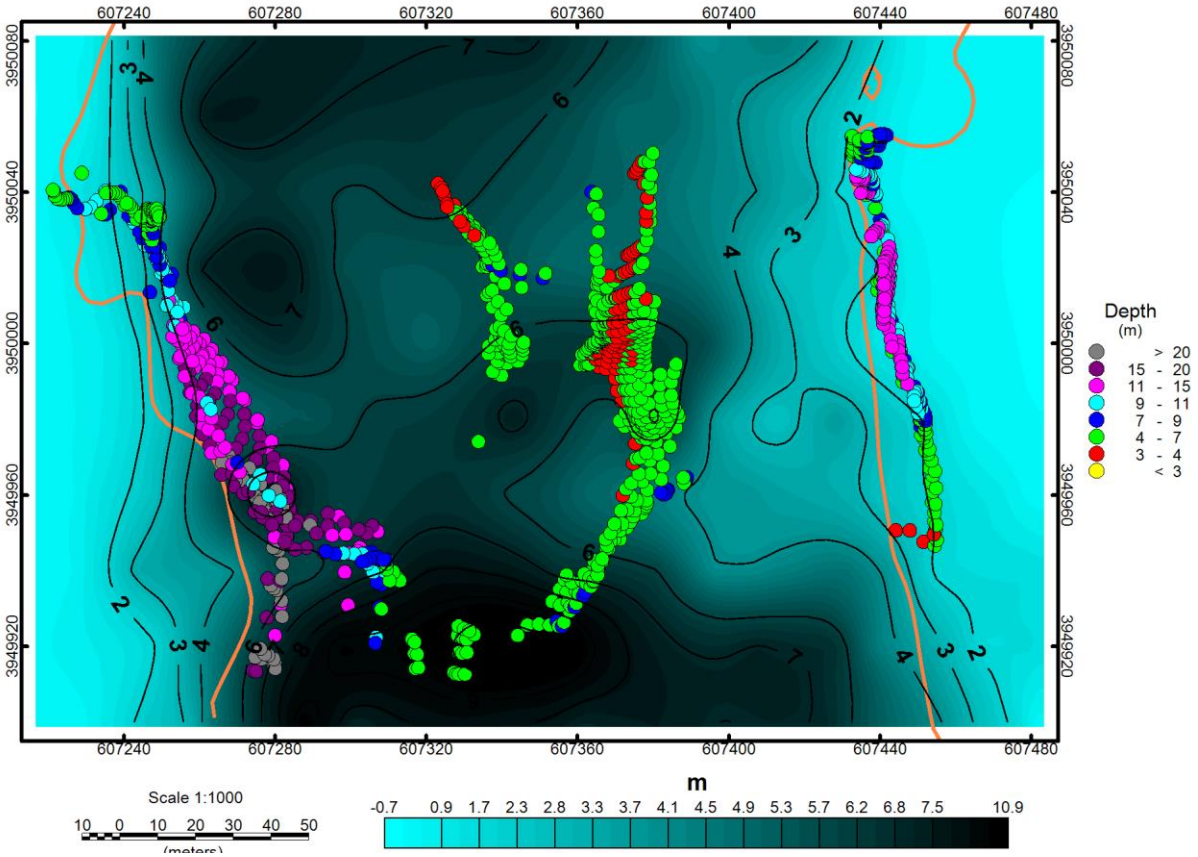
607240
607280
607320
607360
607400
607440
607480
3950080
3950040
3950000
3949960
3949920
Depth
(m)
> 20
15 - 20
11 - 15
9 - 11
7 - 9
4 - 7
3 - 4
< 3
Scale 1:1000
10 0 10 20 30 40 50
(meters)
m
-0.7 0.9 1.7 2.3 2.8 3.3 3.7 4.1 4.5 4.9 5.3 5.7 6.2 6.8 7.5 10.9

b)

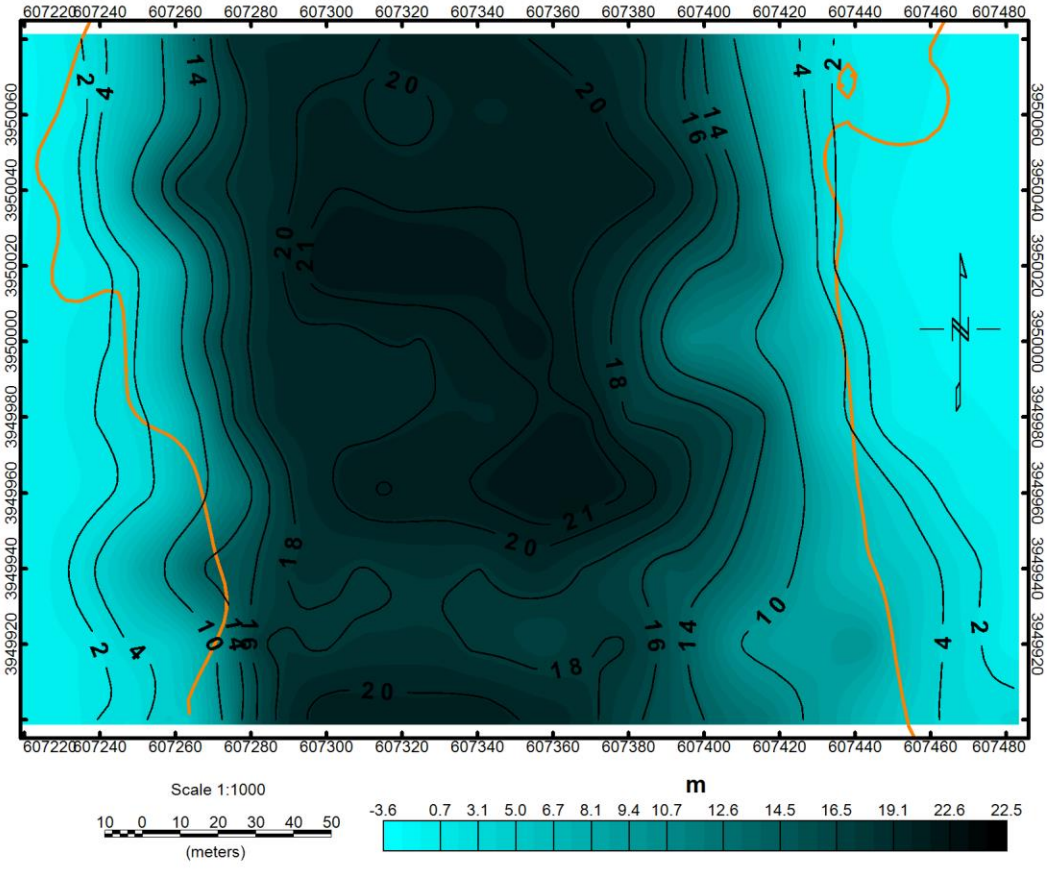
607220
607240
607260
607280
607300
607320
607340
607360
607380
607400
607420
607440
607460
607480
3950060
3950040
3950020
3950000
3949980
3949960
3949940
3949920
N
Scale 1:1000
10 0 10 20 30 40 50
(meters)
m
-3.6 0.7 3.1 5.0 6.7 8.1 9.4 10.7 12.6 14.5 16.5 19.1 22.6 22.5

c)

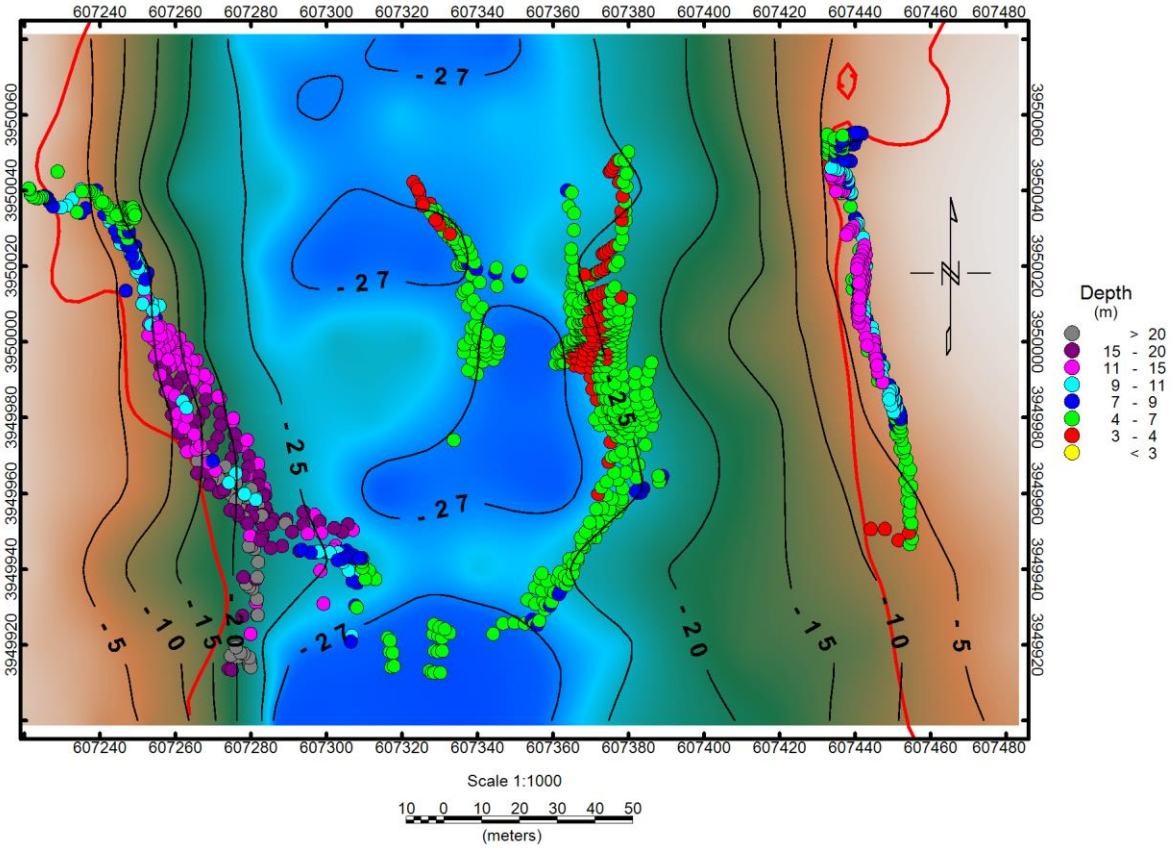
607240
607260
607280
607300
607320
607340
607360
607380
607400
607420
607440
607460
607480
3950060
3950040
3950020
3950000
3949980
3949960
3949940
3949920
-27
-25
-20
-15
-10
-5
N
Depth
(m)
> 20
15 - 20
11 - 15
9 - 11
7 - 9
4 - 7
3 - 4
< 3
Scale 1:1000
10 0 10 20 30 40 50
(meters)


a)


b)

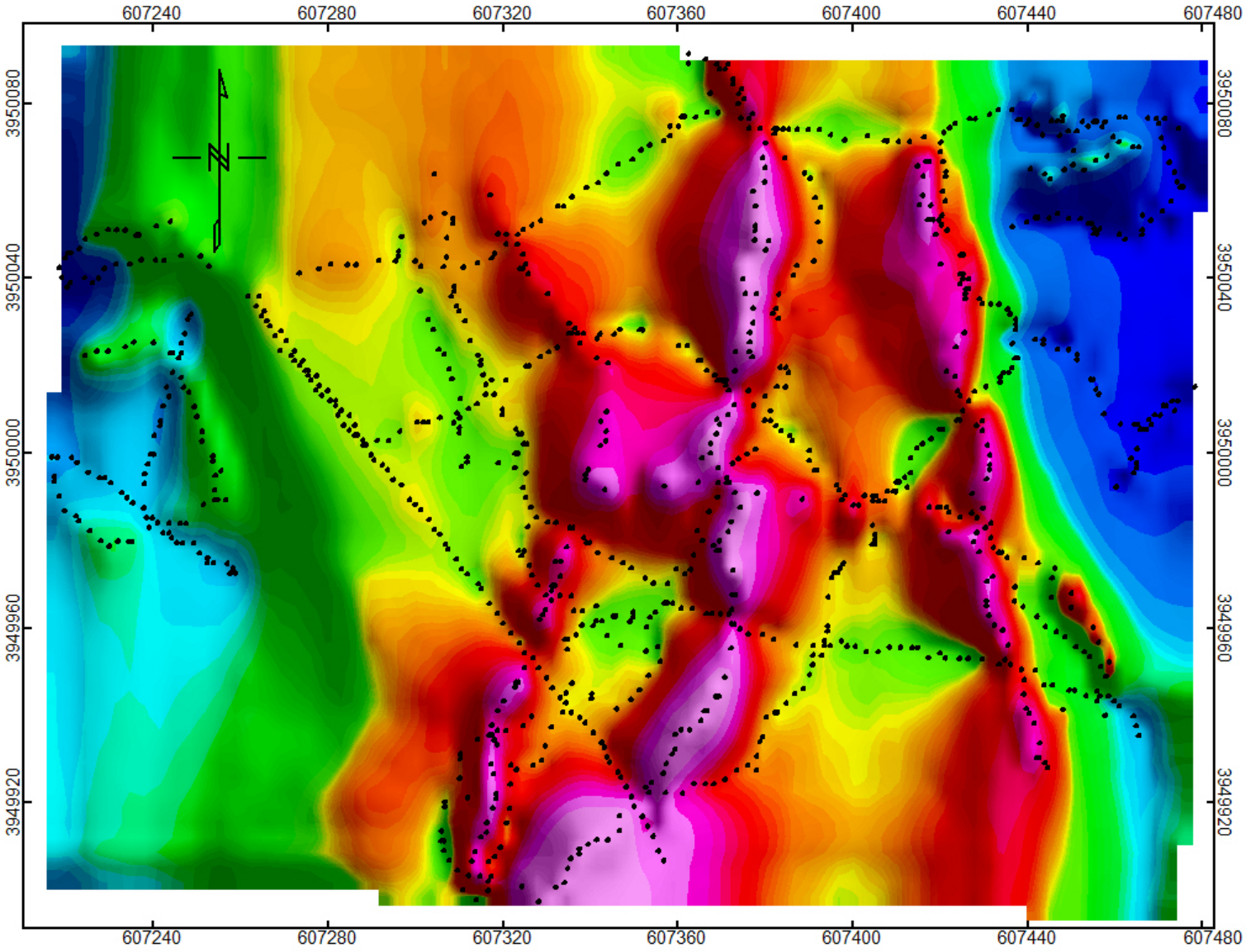
607240
607280
607320
607360
607400
607440
607480
3950080
3950040
3950000
3949960
3949920
Scale 1:1000
10 0 10 20 30 40 50
(meters)
WGS 84 / UTM zone 19S
nT
-201.0 -144.0 -136.7 -126.6 -120.8 -119.8 -118.8 -117.2 -113.9 -87.9

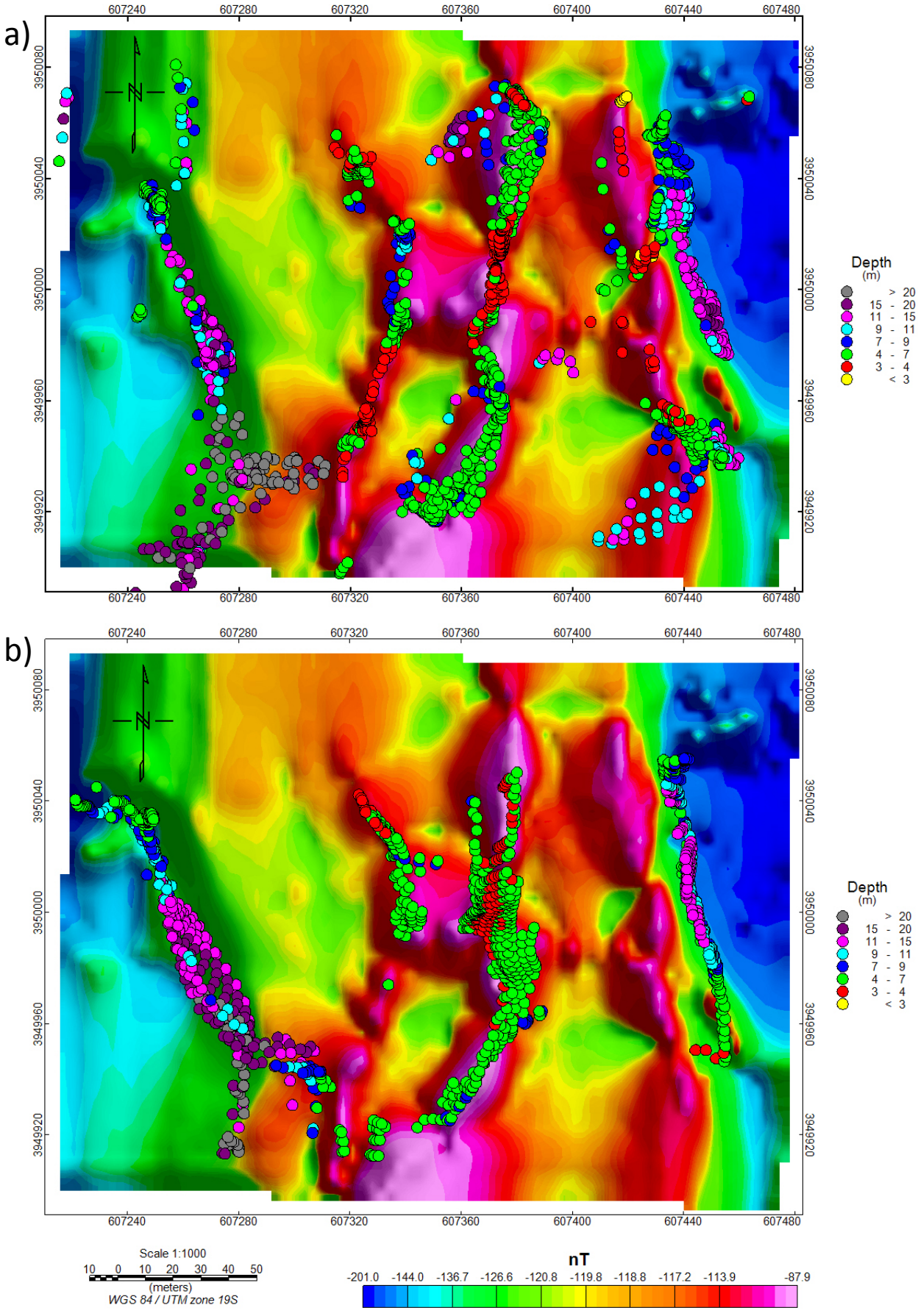
a)
b)
607240
607280
607320
607360
607400
607440
607480
3950080
3950040
3950000
3949960
3949920
Depth
(m)
> 20
15 - 20
11 - 15
9 - 11
7 - 9
4 - 7
3 - 4
< 3
Scale 1:1000
10 0 10 20 30 40 50
(meters)
WGS 84 / UTM zone 19S
nT
-201.0 -144.0 -136.7 -126.6 -120.8 -119.8 -118.8 -117.2 -113.9 -87.9

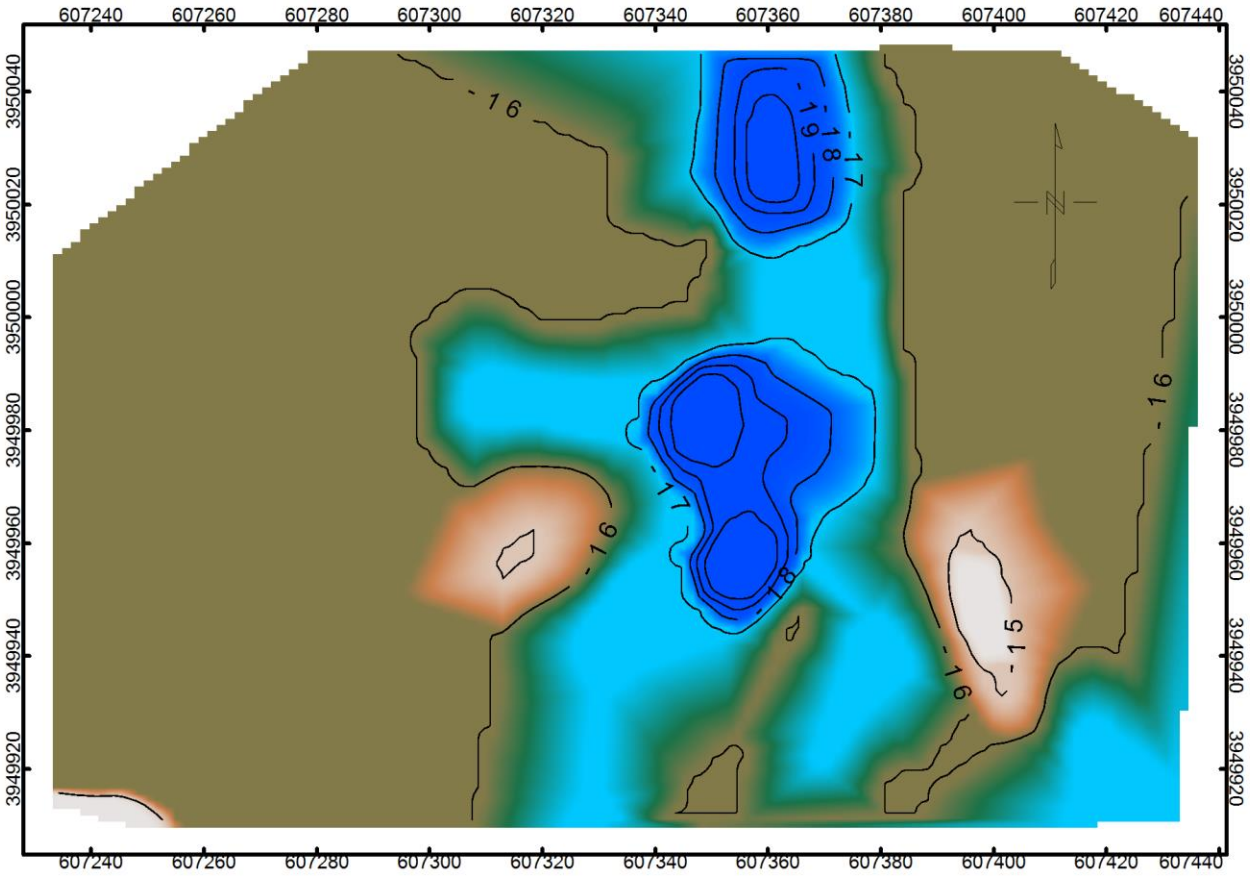

Scale 1:700

10 0 10 20 30 40

(meters)

a)

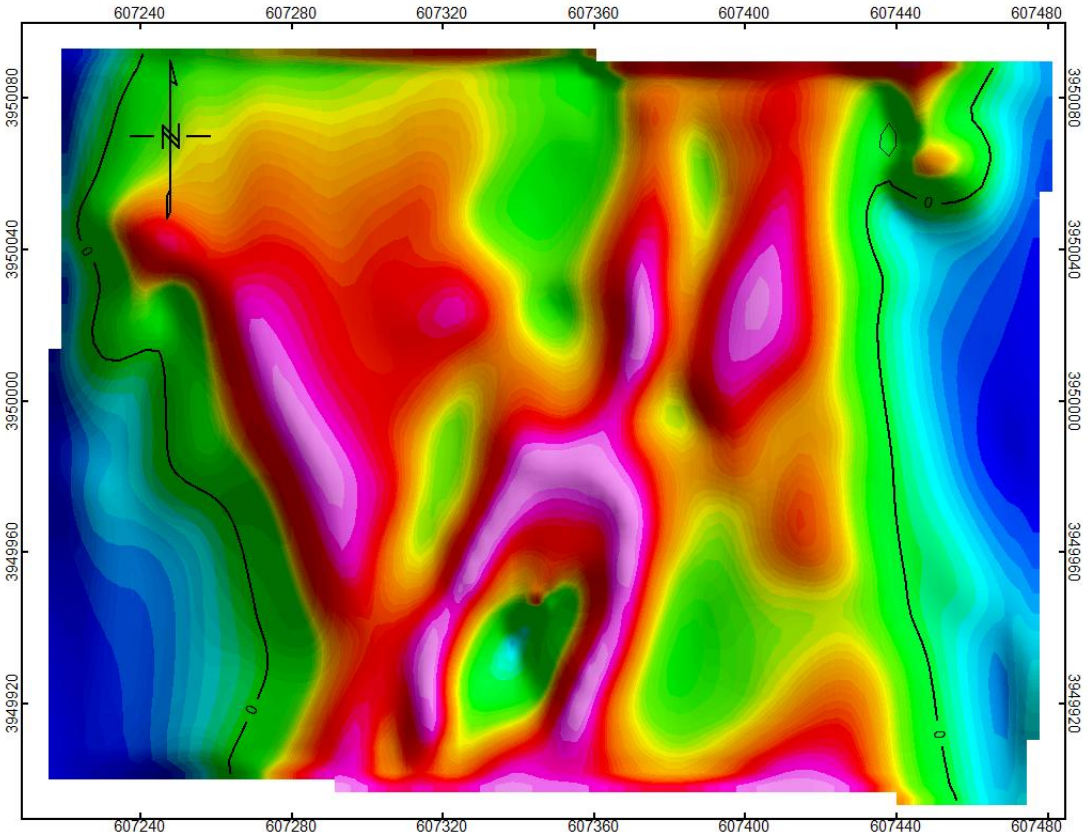

b)

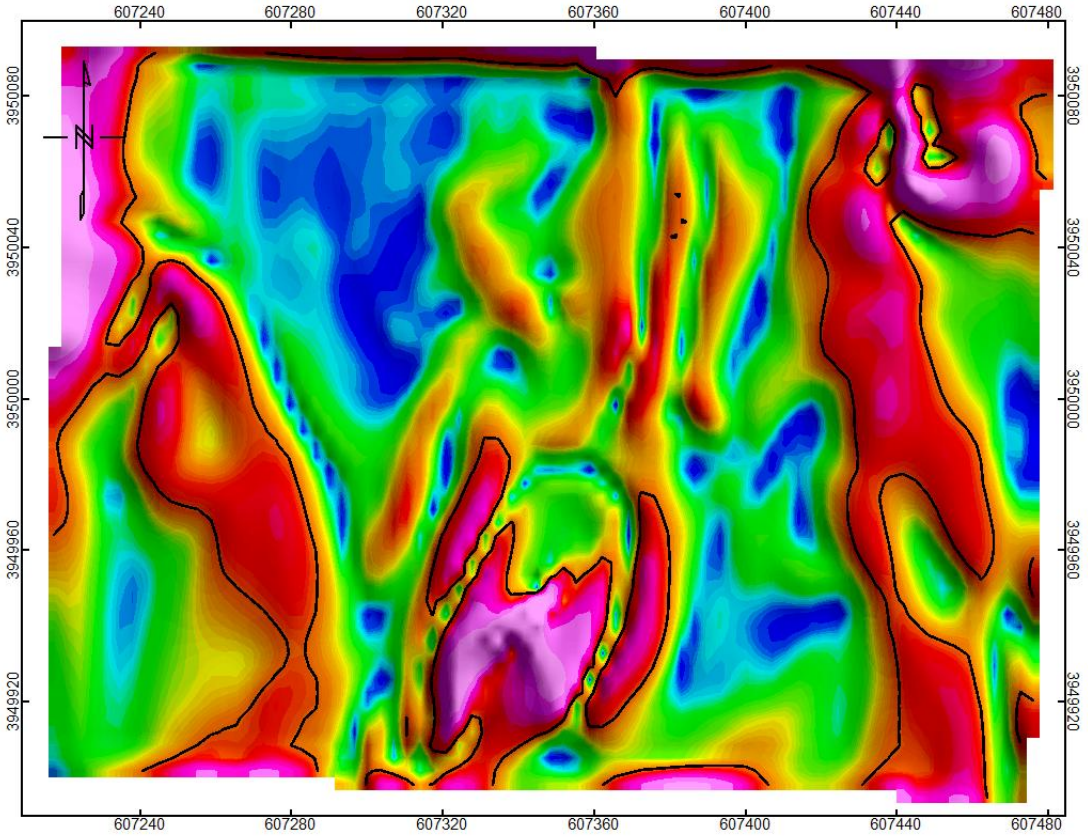

Scale 1:1000

10 0 10 20 30 40 50

(meters)

WGS 84 / UTM zone 19S

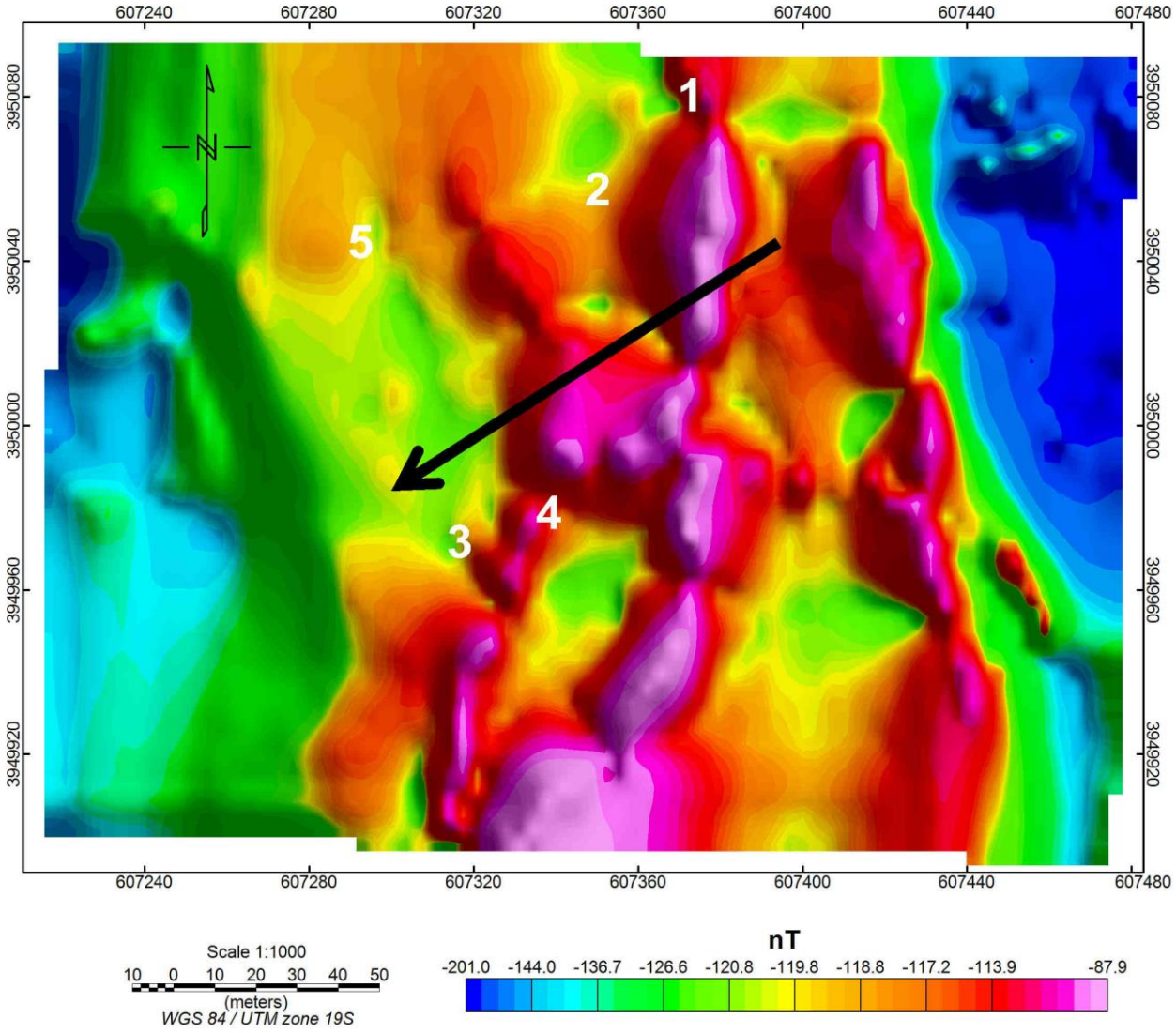
607240
607280
607320
607360
607400
607440
607480
3950080
3950040
3950000
3949960
3949920
N
1
2
3
4
5
Scale 1:1000
10 0 10 20 30 40 50
(meters)
WGS 84 / UTM zone 19S
nT
-201.0 -144.0 -136.7 -126.6 -120.8 -119.8 -118.8 -117.2 -113.9 -87.9

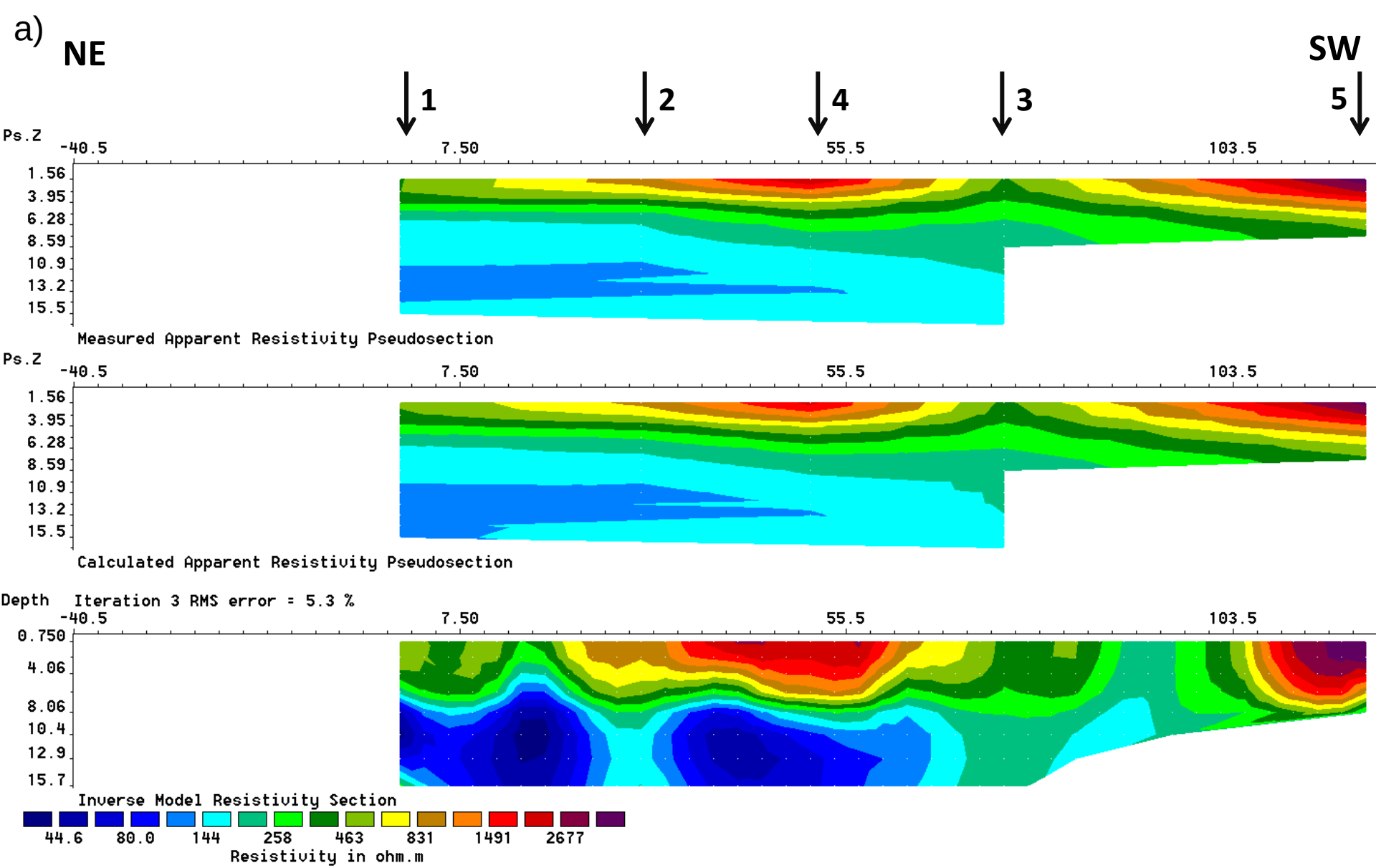
a)
NE
SW
1
2
4
3
5
Ps.Z
-40.5
7.50
55.5
103.5
1.56
3.95
6.28
8.59
10.9
13.2
15.5
Measured Apparent Resistivity Pseudosection
Ps.Z
-40.5
7.50
55.5
103.5
1.56
3.95
6.28
8.59
10.9
13.2
15.5
Calculated Apparent Resistivity Pseudosection
Depth
Iteration 3 RMS error = 5.3 %
-40.5
7.50
55.5
103.5
0.750
4.06
8.06
10.4
12.9
15.7
Inverse Model Resistivity Section
44.6
80.0
144
258
463
831
1491
2677
Resistivity in ohm.m

b)

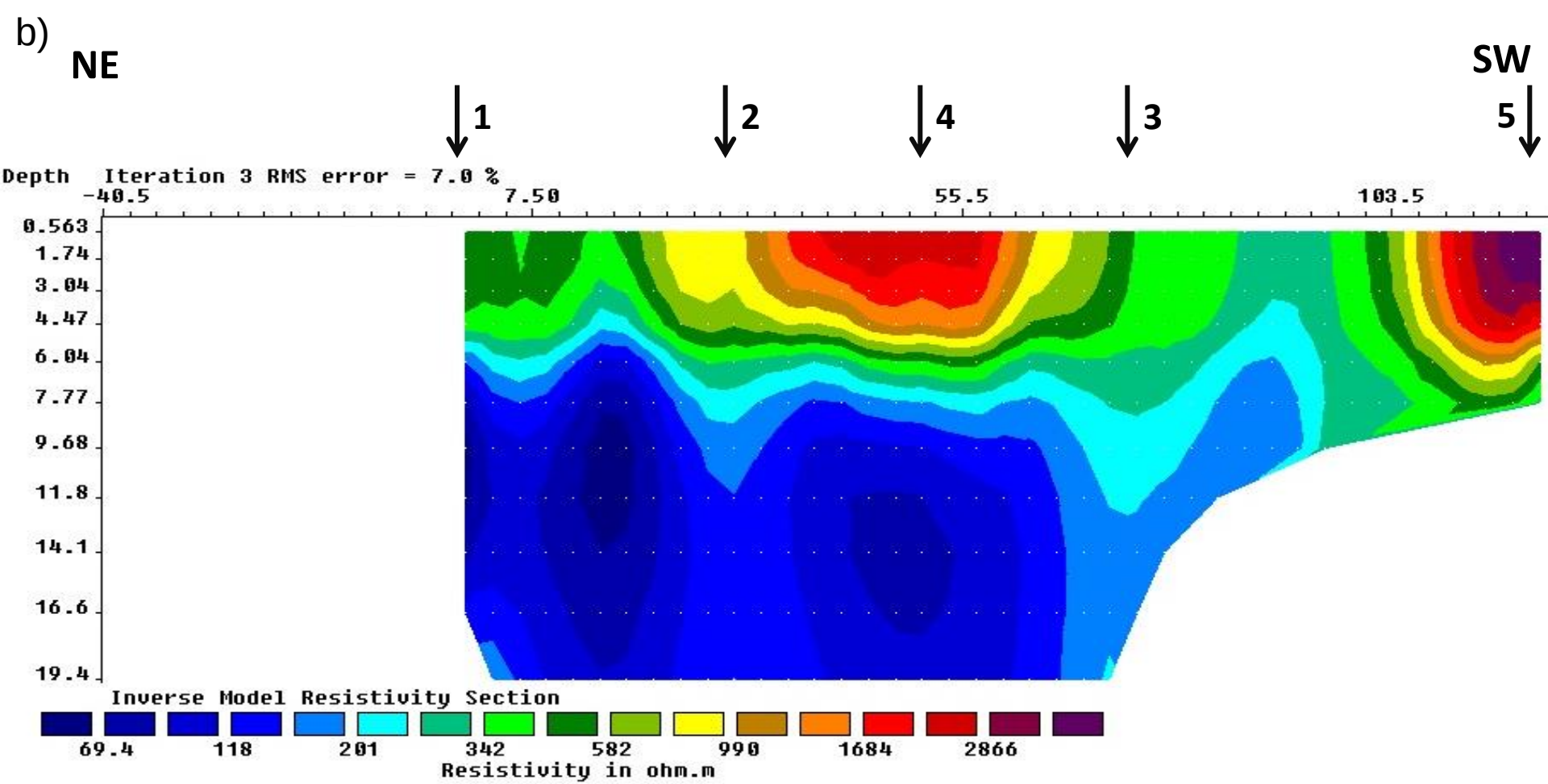
NE
SW
1
2
4
3
5
Depth
Iteration 3 RMS error = 7.0 %
-40.5
7.50
55.5
103.5
0.563
1.74
3.04
4.47
6.04
7.77
9.68
11.8
14.1
16.6
19.4
Inverse Model Resistivity Section
69.4
118
201
342
582
990
1684
2866
Resistivity in ohm.m

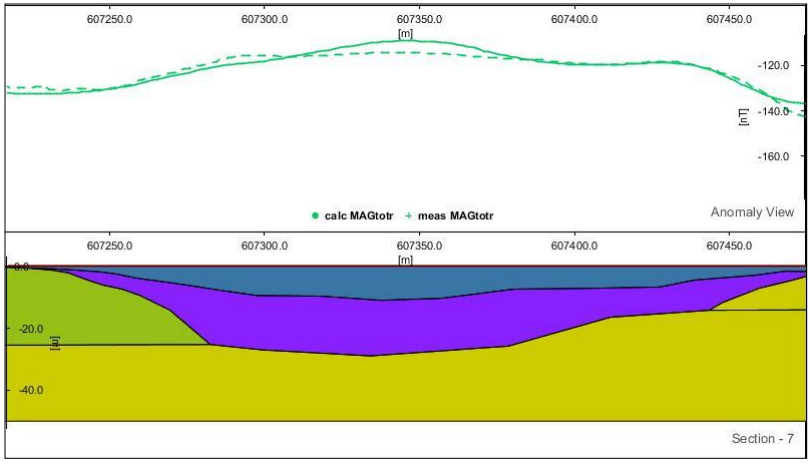
607250.0
607300.0
607350.0
607400.0
607450.0
[m]
-120.0
-140.0
-160.0
[nT]
calc MAGtotr
meas MAGtotr
Anomaly View
0.0
-20.0
-40.0
[m]
Section - 7

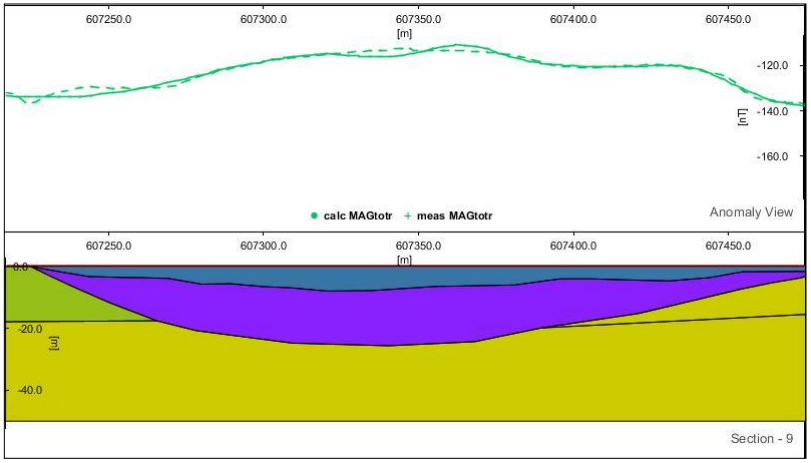
607250.0
607300.0
607350.0
607400.0
607450.0
[m]
-120.0
-140.0
-160.0
[nT]
calc MAGtotr
meas MAGtotr
Anomaly View
0.0
-20.0
-40.0
[m]
Section - 9

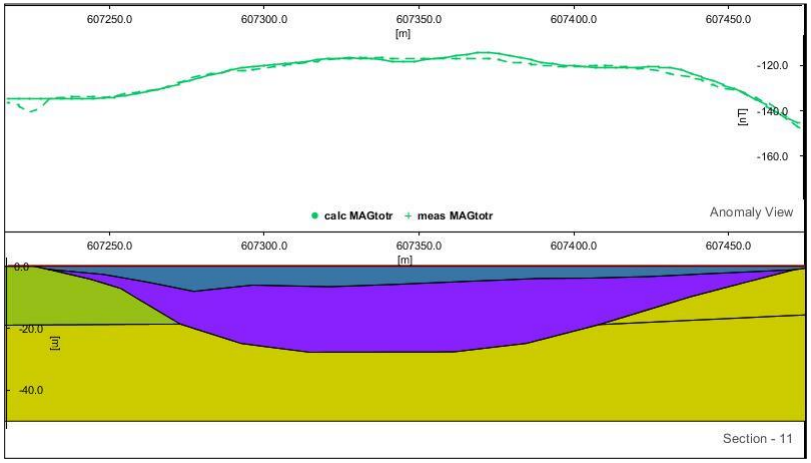
607250.0
607300.0
607350.0
607400.0
607450.0
[m]
-120.0
-140.0
-160.0
[nT]
calc MAGtotr
meas MAGtotr
Anomaly View
0.0
-20.0
-40.0
[m]
Section - 11

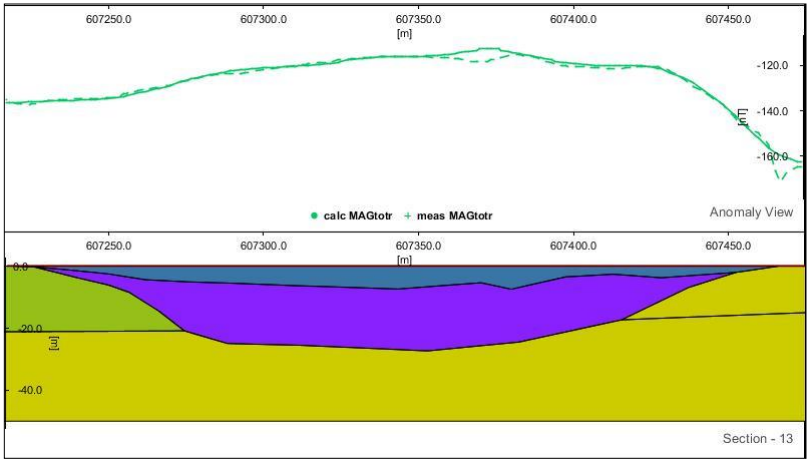
607250.0
607300.0
607350.0
607400.0
607450.0
[m]
-120.0
-140.0
-160.0
[nT]
calc MAGtotr
meas MAGtotr
Anomaly View
0.0
-20.0
-40.0
[m]
Section - 13

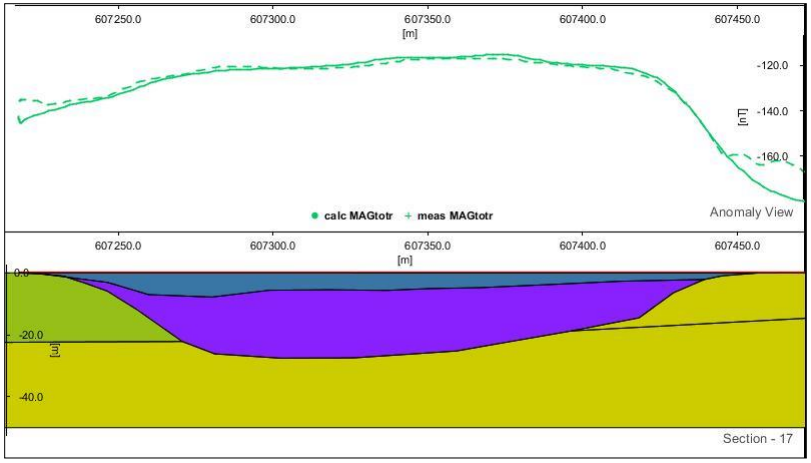
607250.0
607300.0
607350.0
607400.0
607450.0
[m]
-120.0
-140.0
-160.0
[nT]
calc MAGtotr
meas MAGtotr
Anomaly View
0.0
-20.0
-40.0
[m]
Section - 17

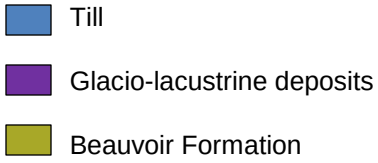
Till
Glacio-lacustrine deposits
Beauvoir Formation

We wish to confirm that there are no known conflicts of interest associated with this publication and there has been no significant financial support for this work that could have influenced its outcome.